Article

Effects of Pre-Strain on the Aging Behavior of Al 7075 Alloy for Hot-Stamping Capability

Seon-Ho Jung [1,2,3], Jongsup Lee [2,*] and Megumi Kawasaki [1,4,*] (iD)

[1] Division of Materials Science and Engineering, Hanyang University, Seoul 04763, Korea; jsh5626@hanyang.ac.kr
[2] Metal Forming Technology R&D Group, Korea Institute of Industrial Technology, Incheon 21999, Korea
[3] Department of Mechanical Engineering, Inha University, Incheon 22212, Korea
[4] School of Mechanical, Industrial & Manufacturing Engineering, Oregon State University, Corvallis, OR 97331, USA
* Correspondence: jongsup@kitech.re.kr (J.L.); megumi.kawasaki@oregonstate.edu (M.K.); Tel: +82-32-8500-316 (J.L.); +1-541-737-4571 (M.K.)

Abstract: The present study investigates the significance of pre-strain on the T6 aging behavior of an Al 7075 alloy for evaluating the applicability of hot stamping. In practice, the alloy was pre-strained up to 15% during solution heat treatment at 480 °C prior to quenching, and artificial aging was conducted at 120 °C. The peak aging time and precipitation behavior were compared with the alloy with pre-straining at room temperature after quenching but immediately before the artificial aging. The results showed that increasing amounts of pre-strain tend to reduce the aging time up to 50% for achieving peak hardness, which is consistent with the alloy at the T6 condition. There is a limitation for the maximum attainable amount of pre-strain of 10% for the homogeneous distribution of strain when the alloy is strained at room temperature (RT) due to the low formability. The pre-strained alloy as hot stamping exhibited lowering of the peak reaction temperatures for dissolution and formation of Guinier–Preston (GP)-Zones and precipitated with increasing amounts of pre-strain towards 15% through the differential scanning calorimetry analysis, thereby confirming the shortening of the peak aging time. The present study confirms the excellent potential of the hot-stamping process to extend the capability of an Al 7075 alloy.

Keywords: Al alloy; artificial aging; hot stamping; precipitation; pre-strain

1. Introduction

Global warming is a serious concern where it is driven in part by the exhaust gases from automotive vehicles. For both fuel economy and emissions control, reducing the weight of car bodies has been a focused issue in the aerospace and automobile industry [1–4]. For weight reduction, the use of lightweight metals, including Al and Mg alloys, is the main consideration by automakers. In particular, the Al 7075 alloy has attracted considerable attention due to its high strength comparable to many steels, thus leading to ultrahigh specific strength, high fracture toughness, and resistance to stress corrosion cracking [5]. For this type of alloy, precipitation hardening is the main strengthening mechanism, whereas the hot workability becomes lower to enhance the strength of the alloy, as was shown in Al–Mg–Si and Al–Zn–Mg alloys [6], and in Al 7150 [7]. In order to overcome the low formability in the alloy, a limited study has suggested the application of a hot-stamping technique for aluminum alloys [8].

In general, hot stamping is a thermomechanical forming technique which provides plastic deformation during solution heat treatment and subsequent quenching while a metal sample is in a forming die. The forming technique has developed for subjecting metals with limited formability,

such as boron steel [9,10]. Specifically, processing by hot stamping provides high strength by inducing the martensitic transformation of the steel by quenching within the die [9–11]. For an Al 7075 alloy, the hot-stamped parts are rapidly quenched to obtain W-temper, and then requires artificial aging cycles of T6 or T7 in order to achieve high strength [8].

Several studies have demonstrated that the aging behavior of an Al 7075 alloy is significantly influenced by pre-straining before the aging treatment. In practice, Kaçar and Güleryüz examined that aging time and temperature, quenching rate, and pre-strain show a critical influence on the strength of Al 7075 alloy [12]. Keci et al. demonstrated that faster quenching rate provides higher yield strength without applying aging treatment, and the highest achieved yield strength was equivalent to the T6 strength of 528 MPa [13].

Importance of pre-straining before aging was demonstrated by Wang et al. where the combination of pre-straining with a two-step aging process improved both the strength and stress corrosion cracking resistance of an Al 7050 alloy [14]. Moreover, both bake-hardening and maximum yield strength was improved by an increasing amount of pre-strain up to 6% before a baking/aging treatment on an Al 7075 alloy [15] and the result is consistent with the baking behavior after pre-straining of an Al–Mg–Si alloy [16]. Furthermore, pre-straining before aging significantly increased the peak aging hardness and shortened the peak aging time of the Al–Mg–Si–Cu alloy [17].

Accordingly, this study was initiated to investigate the significance of pre-strain on the aging behavior of Al 7075-T6 alloy for evaluating the applicability of hot stamping. In order to simulate the hot stamping process, a set of solutionized specimens was tensioned to have different amounts of strain at 480 °C and quenched afterwards. Then, the materials were treated by artificial aging, and the strain homogeneity, hardness, and precipitation behavior were evaluated. Special emphasis was placed on examining these properties in the materials with pre-straining at high temperature as hot-quenching, comparing with the material pre-strained at room temperature (RT) after quenching but prior to aging, so that the feasibility of hot stamping was evaluated for the Al 7075 and similar-class alloys.

2. Experimental Material and Procedure

The present experiments were conducted by using a commercial Al 7075 alloy, which was provided from KAISER® (Oakland, CA, USA) as a sheet with a thickness of 2.0 mm. The chemical composition of the alloy is shown in Table 1. A set of experimental specimens was machined to have the specific dimensions according to the metal testing standard in ASTM-E8 (ASTM International, West Conshohocken, PA, USA) and it is shown in Figure 1, where the longer length of the specimens is parallel to the rolling direction.

Table 1. Chemical composition of Al 7075 alloy (wt. %).

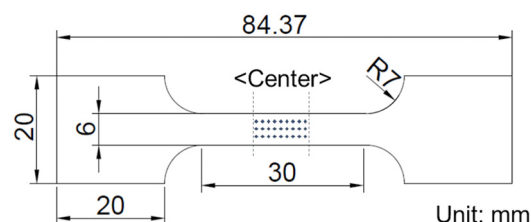| Mg	Zn	Cu	Si	Fe	Mn	Ti	Zr	Cr	V	Etc.
2.39	5.61	1.36	0.095	0.18	0.042	0.032	0.016	0.2	0.011	0.064

Figure 1. Schematic drawing of the experimental specimen where the longer length is parallel to the rolling direction of the as-received sheet.

Simulating a hot-stamping process, the Al 7075 specimens were solution-heat-treated in a chamber for 30 min at 480 °C. Some specimens were strained in tension for 5%, 10%, and 15% at 480 °C by

UTM (i-UT50, EXCELAB, Daejeon, Korea). Then, these were rapidly quenched to attain W-temper by cool water. Afterwards, an artificial aging treatment was conducted at 120 °C in a heat wind circulating oven to achieve the peak age hardening. For comparison purposes, another set of samples were solution-heat-treated for 30 min at 480 °C without straining and quenched, and then followed by pre-straining at RT for 5%, 10%, and 15% in tension before the consistent aging treatment.

The experimental schedules of the heat treatment, quenching, and artificial aging are illustrated in Figure 2 with the pre-straining schedules at (a) 480 °C followed by quenching and (b) RT after quenching. It should be noted that 30 min of the solution heat treatment at $\geq$470 °C is enough to achieve the homogenization in Al 7075 alloy in terms of hardness and electrical conductivity [18]. For reliability of the present procedures, a few samples at each measurement condition were prepared for at least two separate procedures. The homogeneity of strain distribution within the sample gauges was examined immediately after the straining schedules with application of the digital image correlation (DIC) technique [19] by utilizing the ARGUS measuring system (Marlton, NJ, USA) and the DIC software (ARAMIS 3D, GOM mbH, Braunschweig, Germany).
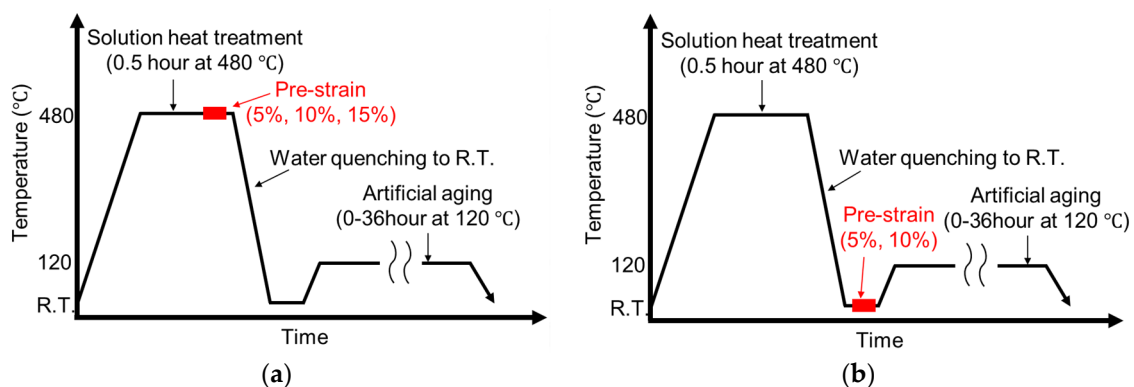

Figure 2. Experimental schedules of the T6 treatment conditions with pre-straining at (**a**) 480 °C as hot-stamping and (**b**) RT after quenching.

Hardness testing was conducted to observe the changes in hardness in the alloy with different amounts and lengths of pre-straining and aging time, respectively. The measurements were operated using a Vickers microhardness tester (HM-100, Mitutoyo, Kanagawa, Japan) with a load of 100 gf and a dwell time of 12 s. An average Vickers microhardness value, Hv, was estimated from the 27 separate measurements with intervals of ~1 mm at the central region of each gauge length. The detailed locations of hardness measurements are shown in Figure 1.

Microstructural characterizations were carried out with transmission electron microscopy (TEM). All TEM micrographs were obtained from a FEI Technai G2 ST-F20 TEM operating under an accelerating voltage of 200 keV. The TEM specimens were prepared by cutting a thin slice with a thickness of ~3.0 μm, punching disk samples with a diameter of 3 mm, and mechanical grinding to a thickness of ~1.5 μm. These disks were then prepared using a precision ion beam cross-section polisher (Gatan 695, Gatan, Pleasanton, CA, USA) and a low voltage Ar ion beam (3 kV) to polish and remove material. During this operation, the specimen stage rotated automatically by $\pm4°$ to prevent beam striations and to ensure uniform polishing.

Thermal analysis was carried out using the differential scanning calorimetry (DSC) system (TA-100, TA Instruments, New Castle, DE, USA). High purity Al 99.9% was used as a reference material. The specimens were heated from 50 to 350 °C at a constant heating rate of 10 °C min^{-1}. The selected conditions of samples were prepared for the DSC testing to have thicknesses of ~0.6 mm with weights of ~20 mg.

3. Results and Discussion

3.1. Strain Distribution with Different Strain Levels in Al 7075 Alloy

One of the critical parameters in the present experiments is the amount and homogeneity of pre-strain before the aging treatment. Thus, the gauge lengths of the Al 7075 specimens shown in Figure 1 have to receive the selected amount of pre-strain homogeneously without the formation of local strain concentrations that lead to necking. Accordingly, the strained gauge surfaces were examined by the DIC system, which collected a data set of strain and displacement during straining. To make the interpretation of the data easier, the data set was presented in color-coded contour strain maps, as shown in Figures 3 and 4 for the Al 7075 with different straining conditions.
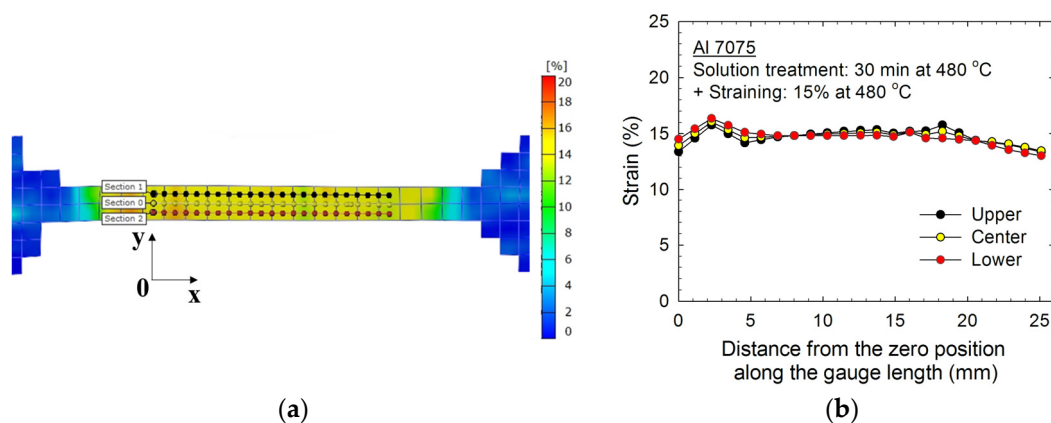

(a)　　　　　　　　　　　　　　　　　　　　　　　　　　　　　　(b)

Figure 3. (**a**) A representative strain map for the specimen strained for 15% at 480 °C, where the measurement locations at three sections of upper, center, and lower are shown in black, yellow, and red dots, respectively, and the individual values of strain are represented by a set of unique color keys; and (**b**) variation of strain versus distance from the zero position at the three separate measurement sections along the gauge length in the Al 7075 after straining for 15% at 480 °C.

For the samples straining at 480 °C, the strain measurements were conducted before and immediately after straining using the DIC system by recording the surface displacements of the selected positions at the upper, center, and lower sections along the gauge lengths by distances of 1 mm. A representative strain map for the Al 7075 specimen strained for 15% at 480 °C is shown in Figure 3a, where the measurement locations for the local strain at the three sections of upper, center, and lower are shown in black, yellow, and red dots, respectively. In the display, the individual values of strain are represented by a set of unique color keys denoting values from 0 to 20% in incremental steps of two. Thus, it is apparent that the strain distribution is reasonably homogeneous in both thickness and length of the sample gauge.

Figure 3b shows the variation of strain with distance from the zero position along the gauge length as shown in Figure 3a for the separate measurement sections of upper, center, and lower in the Al 7075 gauge after straining for 15% at 480 °C. The result confirms the homogeneous distribution of strain for 15% within the gauge length and thickness. The consistent results of homogeneous strain distribution within the gauges are also demonstrated in the alloy when strained for 5% and 10% at 480 °C, thereby indicating the applicability of pre-strain of at least 15% after solution heat treatment at 480 °C during the hot-stamping procedure of the Al 7075 alloy.

Straining at RT, the DIC system enables to correct the data sets of strain and surface displacement by in situ measurements with higher resolutions. The samples are prepared by the solution heat treatment, water quenching, and straining for 5%, 10%, and 15% in tension at RT. Figure 4 shows (a–c) the strain maps and (d–f) the plots of the strain distributions at the upper, center, and lower sections along the gauge lengths of the Al 7075 alloy after straining at RT for 5%, 10%, and 15%, respectively. The individual values of strain are represented by a set of color keys placed in the right of each strain map.

The strain maps in Figure 4a–c demonstrated that the imposed strain was homogeneously distributed along the gauge lengths of the samples after 5% and 10% of straining, whereas there is clear necking at several local regions within the sample gauge after 15% of strain. The homogeneous and heterogeneous distributions of strain are also apparent in the plots shown in Figure 4d–f, where homogeneous straining for 5% and 10% was demonstrated along the gauge lengths and thicknesses, but the non-uniform distribution of strain was observed at the different sections in the sample gauge after strain for 15% at RT. Thus, the results demonstrated a limitation of pre-straining for up to 10% at RT in the present experimental conditions and, more importantly, this limitation in the amount of attainable strain restricts any potential of RT pre-straining for the development of forming techniques, such as bake hardening [14,20] and double thermomechanical treatment [21] of Al 7075 alloy.
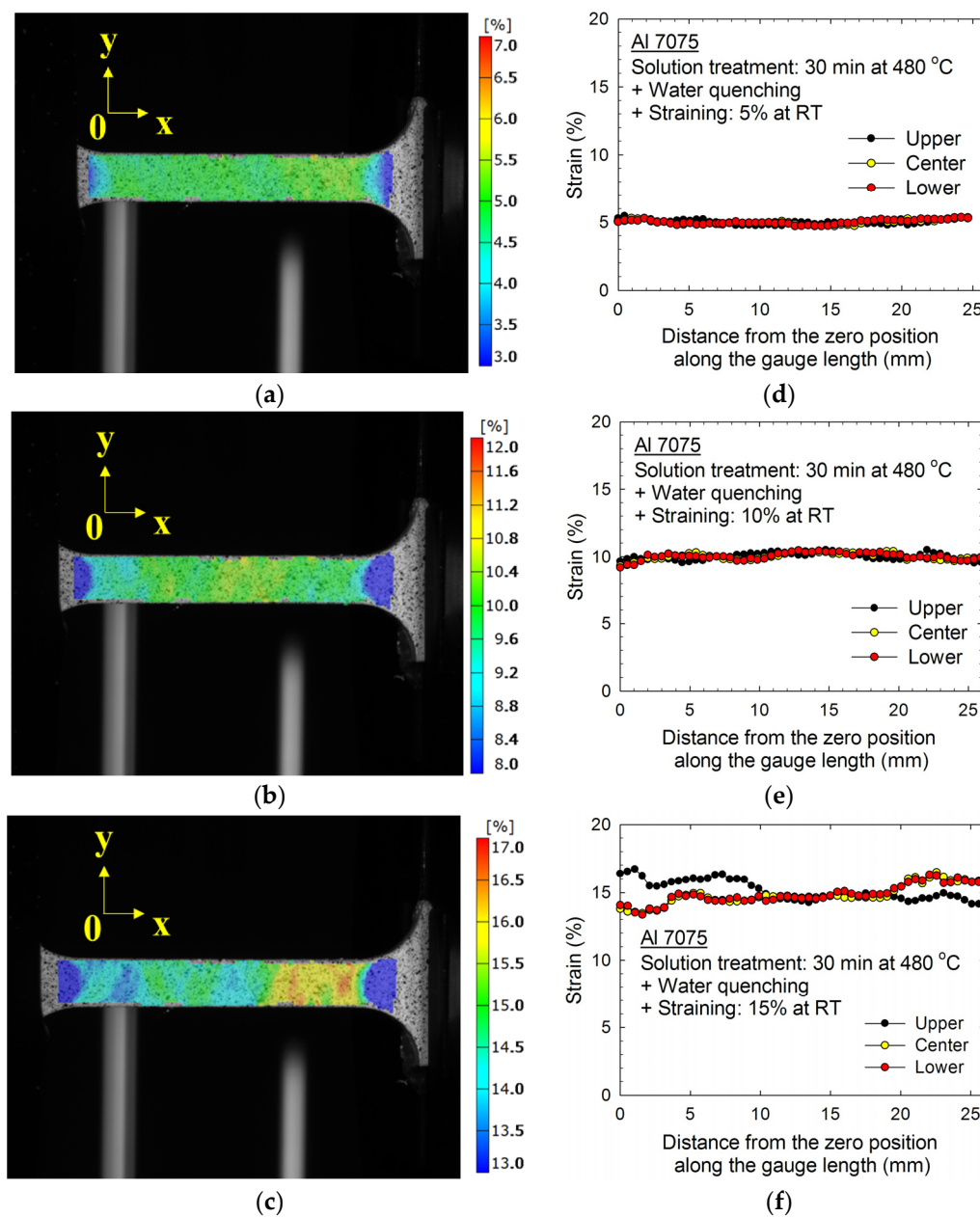

Figure 4. (**a–c**) The strain maps and (**d–f**) the plots of the strain distributions at the upper, center, and lower sections along the gauge lengths of the Al 7075 alloy after straining at RT for 5%, 10%, and 15%, respectively. The individual values of strain are represented by a set of color keys placed in the right of each strain map.

3.2. Peak Aging Hardness and Aging Time

The variations of Vickers microhardness with aging time are shown in Figure 5 for the alloy with different amount of pre-strain at (a) 480 °C and (b) RT. In each plot, there is a datum line of 0% strain indicating the hardness of the material without any pre-straining procedure during the series of heat treatments. Error bars are not included because of very small difference in Hv of ±1 at each testing condition. The sample without pre-strain shows the hardness of Hv ≈88 immediately after quenching prior to aging (0 h of aging time) and the peak aging hardness of Hv ≈180 after aging for 24 h at 120 °C, where the hardness value is consistent with the reference value of 175 for an Al 7075-T6 [22].
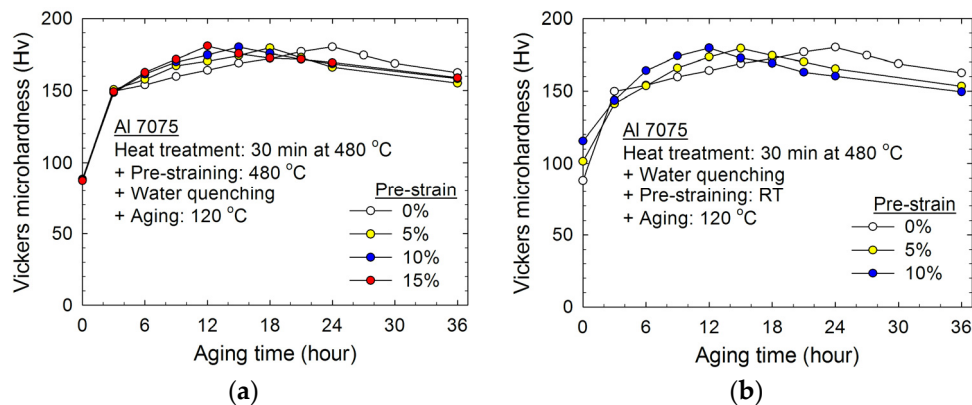

Figure 5. Variations of Vickers microhardness with aging time for the Al 7075 alloy with different amount of pre-strain at (**a**) 480 °C and (**b**) RT.

There are two important findings in Figure 5. Firstly, the hardness values at 0 h of aging time for the pre-strained samples for 5%, 10%, and 15% at 480 °C are consistent with the sample without pre-strain as shown in Figure 5a. On the contrary, the samples immediately after pre-straining at RT recorded the higher hardness to ~100 and ~115 with increasing straining of 5% and 10%, respectively, as shown in Figure 5b. This difference in the hardness values is attributed to the different time schedule of straining in these thermomechanical treatments leading to the extremes in microstructure of the Al alloy. In practice, at the aging time of zero, the pre-strained samples at high temperature consist of as-quenched supersaturated solid solutions. Thus, thermal straining by quenching controls the hardness dominantly since strain hardening may be less effective because of possible dynamic recovery and dynamic polygonization during mechanical straining at high temperature [23]. Therefore, at 0 h of aging, it is reasonable to record the consistent hardness value of ~80 in the alloy without pre-straining and with pre-straining at 480 °C. However, the samples strained at RT passed the stage of supersaturated solid solution before straining and thus show the greater effect of strain hardening by the low-temperature mechanical treatment in comparison with the material strained at high temperature, thereby recording higher hardness with increasing amounts of strain leading to higher dislocation density.

Secondly, all samples with and without pre-straining achieved the consistent peak hardness values of Hv ≈180, whereas there is a clear tendency of reduction in the aging time for achieving the peak hardening with increasing amounts of pre-strain at both temperatures. Specifically, the peak hardness was achieved after 18, 15, and 12 h of aging on the samples with pre-straining at 480 °C for 5%, 10%, and 15%, respectively, and after 15 and 12 h of aging on the samples with RT pre-straining of 5% and 10%, respectively. For better understanding, the optimal aging time for the peak hardness and the amount of pre-strain is summarized in Figure 6. Thus, with the highest amount of pre-straining under the present testing conditions, the total aging time for achieving the peak aging hardness was dramatically reduced for up to 50% compared with the alloy without any pre-straining.
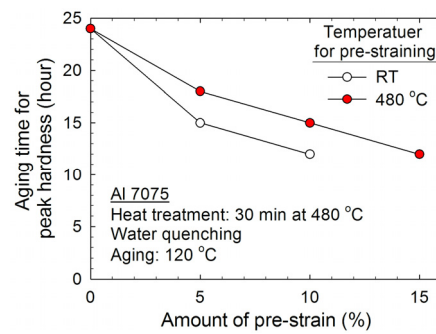
Figure 6. Plot of the optimal aging time for the peak aging hardness versus the amount of pre-strain.

The acceleration in the optimum aging time for the peak hardness is affected by the interaction between crystal defects and precipitated particles. Before the aging treatment, the microstructure of the Al alloy is thermodynamically unstable by quenching and in addition holds high dislocation densities and crystal defects by pre-straining. For such unstable microstructure, the age hardening phenomenon tends to be accelerated due to the increased number of potential precipitation sites and enhanced diffusion rate leading to faster precipitation rate [23]. Thus, it is reasonable to observe the accelerated age hardening effect with increasing amounts of pre-strain in the Al 7075 alloy. Further study for the acceleration of age hardening is studied in the following section.

It should be noted that the artificial aging temperature of 120 °C in the present experiments is sufficiently low so that the certain level of strain hardening remains in the material by only the occurrence of recovery without recrystallization during aging. Therefore, the samples with pre-straining at both 480 °C and RT enabled to exhibit the high hardness value that is equivalent to the Al 7075-T6. The reasonably consistent values of Hv ≈180–200 were demonstrated by double aging and thermomechanical double aging processes with aging at 121 and 171 °C on an AA 7075 alloy [24]. Accordingly, although the pre-straining at RT achieved the peak hardening in slightly shorter time of aging than the pre-strained sample at high temperature, as shown in Figure 6, the RT pre-strain is limited for up to 10%, as was shown in Figure 4 for the Al 7075 alloy. Thus, the results suggest the potential of hot-stamping on the Al 7075 alloy.

3.3. Microstructure and Precipitation Behavior

It is well described that the precipitation sequence of Al–Zn–Mg–Cu alloys is expressed as follows [25]: Super saturated Solid Solution → GP-Zones (GPZs) → metastable η′ phase → stable η phase ($MgZn_2$). This series of Al alloys at the peak aged condition contains the main precipitate of the metastable η′ phase transformed from GPZs, but thereafter the stable η phase is the main precipitate at the over aged condition [26].

The consistent peak hardness value of Hv ≈180 was observed at the optimum aging time for the present experimental alloy with and without pre-strain. Figure 7 shows representative TEM micrographs of the Al 7075 at the peak hardened conditions with (a,b) 0% straining with aging for 24 h (equivalent to the Al 7075-T6) and (c,d) pre-straining for 15% at 480 °C with aging for 12 h, where (a,c) are taken at lower magnifications and (b,d) are taken at higher magnifications. It is apparent that the samples with and without pre-straining showed the reasonably consistent microstructure with homogeneously distributed precipitations at these peak aging conditions. Thus, the precipitates are anticipated as the metastable η′ particles leading to the high hardness, and the pre-strained Al 7075 alloy is expected to show the similar precipitation properties with the Al 7075-T6 alloy under the peak age hardened condition.
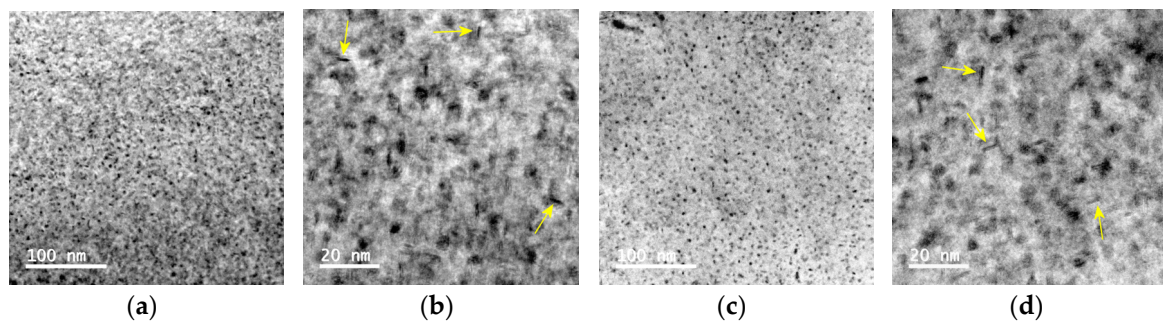
Figure 7. Representative TEM micrographs of the Al 7075 at the peak hardened conditions with (**a**,**b**) 0% straining with aging for 24 h (equivalent to Al 7075-T6); and (**c**,**d**) pre-straining for 15% at 480 °C with aging for 12 h: (**a**,**c**) are taken at lower magnifications and (**b**,**d**) are taken at higher magnifications.

It is important to mention that several elongated ellipsoidal particles are observed with most other particles in a spherical shape and the ellipsoidal particles are indicated by yellow arrows in Figure 7b,d. The appearance of the ellipsoidal particles is due to the higher content of Cu in the Al alloy [27]. It was demonstrated that only spherical precipitates were observed in the Al–Zn–Mg alloy at the peak aging condition, and the atomic prove microanalysis showed evidence of Cu-free in the particles whereas the ellipsoidal particles contained a significant amount of Cu in an Al–Zn–Mg–Cu alloy after age hardening.

Finally, significance of the amount of pre-strain on the precipitation behavior was examined through the DSC analysis for the hot-stamping capability on the Al 7075. It was reported earlier through the DSC examinations that the first endothermic reaction (stage I) at ~200 °C corresponds to the dissolution of the GPZs, the following double exothermic reactions (stages II and III) at ~240 and ~280 °C are attributed to the formation of the η' phase and the transformation of η' into the η phase, respectively, and the final broad endothermic reaction (stage IV) above 300 °C is associated with the growth of the fine η phase whereas these peak-reaction temperatures tend to shift to the higher values with increasing heating rates in the DSC procedure [28,29].

Figure 8 shows the DSC curves for the Al 7075 after a series of aging treatments with pre-straining at (a) 480 °C before quenching and (b) RT after quenching prior to aging, where the both plots include the DSC curve for the Al 7075-T6 without pre-straining for comparison purposes. It is apparent in both plots that there are clear peaks for the reaction stages of I–III where the reaction peak III is generally small [14,27–30]. Thus, all samples demonstrated the dissolution of GPZs at ~195–200 °C and the formation of η' and η at ~225–230 °C and ~245–255 °C, respectively, while there were very weak or unrecognizable peaks indicating the stage IV at ~320 °C for the dissolution of η in the present experimental conditions.
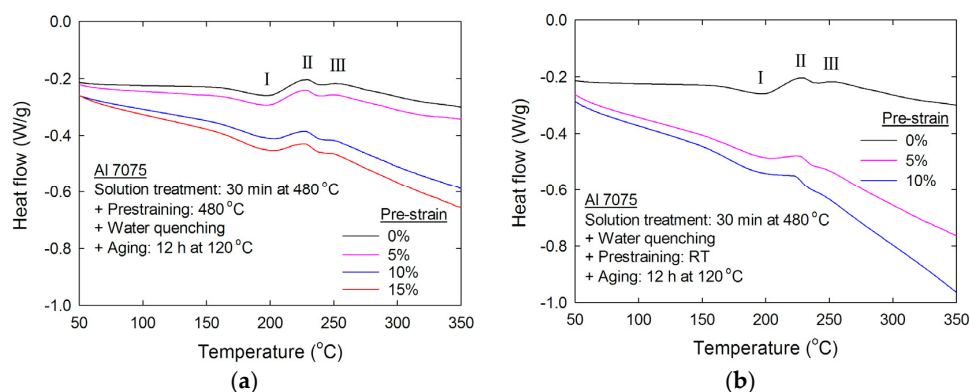

Figure 8. The DSC curves for the Al 7075 with pre-straining at (**a**) 480 °C and (**b**) RT where the plots include the DSC curve for the Al 7075-T6 without pre-straining.

The detailed peak temperatures for each reaction stage were summarized in terms of the amount of pre-strain, and the result is shown in Figure 9 where the upper two lines show the peak temperatures attributing to the stage III, and the center two lines and the lower two lines describe the peak temperatures for the stages II and I, respectively. Although the differences are small, there is a tendency of lowering peak temperature with increasing amounts of pre-strain at both pre-straining temperatures at all precipitation reaction stages.

This tendency is anticipated especially under the present conditions of solution treatment and aging temperatures together with the amount of straining. An earlier report demonstrated by TEM that there are two types of GPZs in 7xxx series Al alloys where GPZ-I is formed over a wide range of aging temperature, including both natural and artificial aging temperatures and independently of quenching temperature, and GPZ-II are formed after quenching from temperatures at >450 °C followed by aging at >70 °C [31]. The GPZ-II is assumed to be the vacancy-rich clusters by quenching [32], and these are easily annihilated in the dislocations produced in the pre-straining process. Thus, the samples with higher dislocation densities can show the accelerated dissolution of GPZs leading to lower peak temperatures for the stage I in the DSC plots. Moreover, the dislocations also provide the heterogeneous nucleation sites for precipitations, and thus such high dislocation density may work also for the fast diffusion passes for precipitation elements during the aging process. It is also reasonable to note that the growth of precipitations may be limited by interaction with dislocations nucleating ledges at the precipitates. Thereby, in the DSC measurements, lower temperature is enough for the precipitates to form, and therefore the shifts of peaks II and III to the lower temperatures are observed in the samples containing higher dislocation densities by pre-straining.

Accordingly, in the present experimental conditions, the samples with pre-straining contain higher dislocation densities and, it is especially apparent in the samples with the highest straining for 15% at 480 °C and 10% at RT. These pre-strained samples show the lowest peak temperatures at all three reaction stages I–III in the present experiments. Considering a potential of further increase in the pre-strain amount at 480 °C, the present experiments conclude the excellent potential of hot stamping to extend the capability of an Al 7075 alloy.

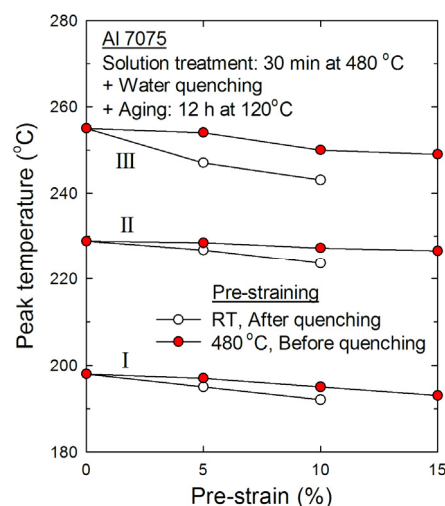**Figure 9.** The peak reaction temperatures for separate precipitation reaction stages I–III with the amount of pre-strain at 480 °C and RT on the Al 7075.

4. Summary and Conclusions

1. The present study examined the effect of pre-straining on the aging behavior of an Al 7075 alloy for evaluating the applicability of the hot-stamping technique. The general age hardening procedures were utilized with addition of straining at the end of the solution heat treatment. The strain homogeneity, hardness, microstructure, and precipitation reactions of the pre-strained

samples were analyzed and compared with the alloy after the consistent aging treatment with pre-straining at RT immediately after quenching.

2. Homogeneous distribution of straining was observed throughout the gauge lengths for at least up to 15% at 480 °C before quenching, whereas there was a localized straining leading to necking at the gauge of the alloy after straining for 15% at RT. In terms of metal forming, the high applicable amount and homogeneity of strain is essential, and thus the result demonstrated the potential of hot-stamping for a forming process of the Al alloy.

3. The aging time for achieving the peak hardness was dramatically reduced for 50% when the samples are pre-strained for the highest amounts of 15% and 10% at high temperature and RT, respectively, in comparison with the alloy in T6 without pre-straining.

4. The peak hardness after pre-straining was consistent with the hardness of Al 7075-T6, and the reasonably similar microstructure was observed by the TEM analysis between the samples at peak aging. The DSC analysis demonstrated the accelerated reactions leading to lower reaction temperatures for GPZs and precipitates in the alloy with increasing amounts of pre-strain producing higher dislocation densities in the Al 7075 alloy. The results support the accelerated peak aging time for the alloy with pre-straining.

Author Contributions: Jongsup Lee conceived and designed the experiments; Seon-Ho Jung performed the experiments; Seon-Ho Jung, Jongsup Lee and Megumi Kawasaki analyzed the data; Megumi Kawasaki wrote the paper.

Conflicts of Interest: The authors declare no conflict of interest.

References

1. Immarigeon, J.-P.; Holt, R.T.; Koul, A.K.; Zhao, L.; Wallace, W.; Beddoes, J.C. Lightweight materials for aircraft applications. *Mater. Charact.* **1995**, *35*, 41–67. [CrossRef]

2. Miller, W.S.; Zhuanga, L.; Bottema, J.; Wittebrood, A.J.; de Smet, P.; Haszler, A.; Vieregg, A. Recent development in aluminium alloys for the automotive industry. *Mater. Sci. Eng. A* **2000**, *280*, 37–49. [CrossRef]

3. Williams, J.C.; Starke, E.A., Jr. Progress in structural materials for aerospace systems. *Acta Mater.* **2003**, *51*, 5775–5799. [CrossRef]

4. Goede, M.; Stehlin, M.; Rafflenbeul, L.; Kopp, G.; Beeh, E. Super Light Car—Lightweight construction thanks to a multi-material design and function integration. *Eur. Transp. Res. Rev.* **2009**, *1*, 5–10. [CrossRef]

5. Clinch, M.R.; Daval, R.; Harris, S.J.; Hepples, W.; Holroyd, N.J.H.; Lawday, M.J.; Noble, B. A microstructural engineering-based approach to 7xxx series alloy optimization. *Mater. Forum* **2004**, *28*, 145–151.

6. McQueen, H.J.; Celliers, O.C. Application of hot workability studies to extrusion processing. Part III: Physical and mechanical metallurgy of Al-Mg-Si and Al-Zn-Mg alloys. *Can. Metall. Q.* **1997**, *36*, 73–86.

7. Jin, N.; Zhang, H.; Han, Y.; Wu, W.; Chen, J. Hot deformation behavior of 7150 aluminum alloy during compression at elevated temperature. *Mater. Charact.* **2009**, *60*, 530–536. [CrossRef]

8. Harrison, N.R.; Luckey, S.G. Hot stamping of a B-pillar outer from high strength aluminum sheet AA7075. *SAE Int. J. Mater. Manuf.* **2014**, *7*, 567–573. [CrossRef]

9. Hossein, K.; Tekkaya, A.E. A review on hot stamping. *J. Mater. Process. Technol.* **2010**, *210*, 2103–2118.

10. Neugebauer, R.; Schieck, F.; Rautenstrauch, A.; Bach, M. Hot sheet metal forming: The formulation of graded component characteristics based on strategic temperature management for tool-based and incremental forming operations. *CIRP J. Manuf. Sci. Technol.* **2011**, *4*, 180–188. [CrossRef]

11. Merklein, M.; Lechler, J. Investigation of the thermo-mechanical properties of hot stamping steels. *J. Mater. Process. Technol.* **2006**, *177*, 452–455. [CrossRef]

12. Kaçar, R.; Güleryüz, K. Effect of quenching rate and pre-strain on the strain ageing behaviors of 7075 aluminum alloys. *Mater. Res.* **2015**, *18*, 328–333. [CrossRef]

13. Keci, A.; Harrison, N.R.; George Luckey, S. *Experimental Evaluation of the Quench Rate of AA7075*; SAE Technical Paper 2014-01-0984; SAE International: Warrendale, PA, USA, 2014. [CrossRef]

14. Wang, D.; Ni, D.R.; Ma, Z.Y. Effect of pre-strain and two-step aging on microstructure and stress corrosion cracking of 7050 alloy. *Mater. Sci. Eng. A* **2008**, *494*, 360–366. [CrossRef]

15. Dehghani, K.; Nekahi, A.; Mirzaie, M.A.M. Optimizing the bake hardening behavior of Al7075 using response surface methodology. *Mater. Des.* **2010**, *31*, 1768–1775. [CrossRef]

16. Birol, Y. Pre-straining to improve the bake hardening response of a twin-roll cast Al–Mg–Si alloy. *Scr. Mater.* **2005**, *52*, 169–173. [CrossRef]

17. Yin, D.; Xiao, Q.; Chen, Y.; Liu, H.; Yi, D.; Wang, B.; Pan, S. Effect of natural ageing and pre-straining on the hardening behaviour and microstructural response during artificial ageing of an Al–Mg–Si–Cu alloy. *Mater. Des.* **2016**, *95*, 329–339. [CrossRef]

18. Andreatta, F.; Terryn, H.; de Wit, J.H.W. Effect of solution heat treatment on galvanic coupling between intermetallics and matrix in AA7075-T6. *Corros. Sci.* **2003**, *45*, 1733–1746. [CrossRef]

19. McCormick, N.; Lord, J. Digital image correlation. *Mater. Today* **2010**, *13*, 52–54. [CrossRef]

20. De, A.K.; de Blauwe, K.; Vandeputte, S.; de Cooman, B.C. Effect of dislocation density on the low temperature aging behavior of an ultra low carbon bake hardening steel. *J. Alloys Compd.* **2000**, *310*, 405–410. [CrossRef]

21. El-Baradie, Z.M.; El-Sayed, M. Effect of double thermomechanical treatments on the properties. *J. Mater. Process. Technol.* **1996**, *62*, 76–80. [CrossRef]

22. ASM International. *Metals Handbook, Vol. 2: Properties and Selection: Nonferrous Alloys and Special-Purpose Materials*, 10th ed.; ASM International: Warrendale, PA, USA, 1990; ISBN 978-0-87170-378-1.

23. Rajan, T.V.; Sharma, C.P.; Sharma, A. *Heat Treatment: Principles and Techniques*; PHI Learning Pvt. Ltd.: New Delhi, India, 2011.

24. Emani, S.V.; Benedyk, J.; Nash, P.; Chen, D. Double aging and thermomechanical heat treatment of AA7075 aluminum alloy extrusions. *J. Mater. Sci.* **2009**, *44*, 6384–6391. [CrossRef]

25. Degischer, H.P.; Lacom, W.; Zahra, A.; Zahra, C.Y. Decomposition processes in an Al-5% Zn-1% Mg alloy. II. Electronmicroscopic investigations. *Z. Metallk.* **1980**, *71*, 231–238.

26. Sha, G.; Cerezo, A. Early-stage precipitation in Al–Zn–Mg–Cu alloy (7050). *Acta Mater.* **2004**, *52*, 4503–4516. [CrossRef]

27. Chinh, N.Q.; Lendvai, J.; Ping, D.H.; Hono, K. The effect of Cu on mechanical and precipitation properties. *J. Alloys Compd.* **2004**, *378*, 52–60. [CrossRef]

28. Lloyd, D.J.; Chaturvedi, M.C. A calorimetric study of aluminium alloy AA-7075. *J. Mater. Sci.* **1982**, *17*, 1819–1824. [CrossRef]

29. García-cordovilla, C.; Louis, E. Kinetics of retrogression in Al-Zn-Mg-(Cu) alloys. *Metall. Trans. A* **1990**, *21*, 2277–2280. [CrossRef]

30. Viana, F.; Pinto, A.M.P.; Santos, H.M.C.; Lopes, A.B. Retrogression and re-aging of 7075 aluminum alloy: Microstructural characterization. *J. Mater. Process. Technol.* **1999**, *92–93*, 54–59. [CrossRef]

31. Berg, L.K.; Gjønnes, J.; Hansen, V.; Li, X.Z.; Knutson-Wedel, M.; Waterloo, G.; Schryvers, D.; Wallenberg, L.R. GP-zones in Al–Zn–Mg alloys and their role in artificial aging. *Acta Mater.* **2001**, *49*, 3443–3451. [CrossRef]

32. Katz, Z.; Ryum, N. Precipitation kinetics in Al-alloys. *Scr. Metall.* **1981**, *15*, 265–268. [CrossRef]